HHS Public Access

Author manuscript

Toxicol Appl Pharmacol. Author manuscript; available in PMC 2018 March 19.

Published in final edited form as:

Toxicol Appl Pharmacol. 2011 November 15; 257(1): 74–83. doi:10.1016/j.taap.2011.08.020.

Use of human stem cell derived cardiomyocytes to examine sunitinib mediated cardiotoxicity and electrophysiological alterations

J.D. Cohen[a], **J.E. Babiarz**[a], **R.M. Abrams**[a], **L. Guo**[a], **S. Kameoka**[a], **E. Chiao**[a], **J. Taunton**[b], and **K.L. Kolaja**[a,*]

[a]Early and Investigative Safety, Nonclinical Safety, Hoffmann-La Roche, 340 Kingsland Street, Nutley, NJ 07110 USA

[b]Howard Hughes Medical Institute, Cellular and Molecular Pharmacology, University California San Francisco, San Francisco, CA 94158 USA

Abstract

Sunitinib, an oral tyrosine kinase inhibitor approved to treat advanced renal cell carcinoma and gastrointestinal stroma tumor, is associated with clinical cardiac toxicity. Although the precise mechanism of sunitinib cardiotoxicity is not known, both the key metabolic energy regulator, AMP-activated protein kinase (AMPK), and ribosomal S 6 kinase (RSK) have been hypothesized as causative, albeit based on rodent models. To study the mechanism of sunitinib-mediated cardiotoxicity in a human model, induced pluripotent stem cell-derived cardiomyocytes (iPSC-CMs) having electrophysiological and contractile properties of native cardiac tissue were investigated. Sunitinib was cardiotoxic in a dose-dependent manner with an IC_{50} in the low micromolar range, observed by a loss of cellular ATP, an increase in oxidized glutathione, and induction of apoptosis in iPSC-CMs. Pretreatment of iPSC-CMs with AMPK activators AICAR or metformin, increased the phosphorylation of pAMPK-T172 and pACC-S79, but only marginally attenuated sunitinib mediated cell death. Furthermore, additional inhibitors of AMPK were not directly cytotoxic to iPSC-CMs up to 250 μM concentrations. Inhibition of RSK with a highly specific, irreversible, small molecule inhibitor (RSK-FMK-MEA) did not induce cytotoxicity in iPSC-CMs below 250 μM. Extensive electrophysiological analysis of sunitinib and RSK-FMK-MEA mediated conduction effects were performed. Taken together, these findings suggest that inhibition of AMPK and RSK are not a major component of sunitinib-induced cardiotoxicity. Although the exact mechanism of cardiotoxicity of sunitinib is not known, it is likely due to inhibition of multiple kinases simultaneously. These data highlight the utility of human iPSC-CMs in investigating the potential molecular mechanisms underlying drug-induced cardiotoxicity.

Keywords

Sunitinib; Human stem cell derived cardiomyocytes; Induced pluripotent stem cells; AMPK; RSK; Cardiotoxicity

*Corresponding author at: Bldg 100–325, Hoffmann-La Roche, 340 N Kingsland St, Nutley NJ 07110 USA. Fax: +1 973 235 4710.

Supplementary materials related to this article can be found online at doi:10.1016/j.taap.2011.08.020.

Introduction

Tyrosine kinase-targeted therapies have revolutionized the treatment of a variety of cancers. Targeted inhibitors of kinases have improved antitumor efficacy and have fewer toxic side-effects, compared to traditional chemotherapy, but have been implicated in causing serious adverse cardiac events (Di Lorenzo et al., 2009; Force and Kolaja, 2011; Menna et al., 2008; Motzer et al., 2007; Orphanos et al., 2009). Sunitinib malate (Sutent; Pfizer) is a multitargeted tyrosine kinase inhibitor that inhibits both tumor cell proliferation and angiogenesis and is approved to treat advanced renal cell carcinoma and gastrointestinal stromal tumours. However, clinically observed serious cardiac adverse events associated with sunitinib include a high incidence of hypertension, cardiac left ventricular systolic dysfunction, and congestive heart failure (Chu et al., 2007; Di Lorenzo et al., 2009; Faivre et al., 2007; Telli et al., 2008). The exact mechanism of this cardiotoxicity is not known but has been broadly attributed to the lack of kinase selectivity of sunitinib, which in a competitive binding assay bound 57 of the 317 kinases tested (18%) at the clinically relevant dose of 0.1 μM (Karaman et al., 2008). Similar to other tyrosine kinase inhibitors (TKIs), the lack of selectivity of sunitinib makes it challenging to pinpoint whether there are specific molecular target(s) that are the critical mediators of cardiotoxicity. In addition to off-target kinase inhibition by TKIs, the interaction with non-kinase targets should also be considered. For example, imatinib (Gleevec; Novartis) is a more selective kinase inhibitor than sunitinib, binding only 10 of the 317 kinases tested with K_d values less than 0.1 μM (Karaman et al., 2008), but binds to non-kinase targets including NQO2 and BCRP (Bantscheff et al., 2007; Meissner et al., 2006).

Due to its role in energy homeostasis, AMP-activated protein kinase (AMPK) has been suggested to be a mediator of sunitinib cardiotoxicity (Force et al., 2007). Depletion of intracellular ATP and increased AMP activates AMPK (α, β, γ subunits) which stimulates catabolic pathways and suppresses non-essential ATP-consuming processes (Kudo et al., 1995, 1996). The rhythmic contraction of cardiac tissues requires a constant, stable source of energy, leaving a limited reserve of ATP. Thus, inhibition of AMPK could disrupt a cardiomyocyte's ability to adapt to energy demands leading to deleterious consequences (Force et al., 2007).

In rodent models of drug-induced cardiotoxicity, conflicting evidence for the role of AMPK in mediating sunitinib induced cardiotoxicity have been reported. In neonatal rat ventricular myocytes (NRVM), sunitinib induced apoptosis, depleted ATP, and led to the release of lactate dehydrogenase (LDH) (Hasinoff et al., 2008; Kerkela et al., 2009). Pretreatment with either AMPK activator, aminoimidazole carboxamide ribonucleotide (AICAR) (Kerkela et al., 2009) or metformin (Hasinoff et al., 2008) in NRVMs failed to attenuate sunitinib cardiotoxicity, and did not reverse the inhibition of p-ACC by sunitinib (AICAR pretreatment) (Kerkela et al., 2009); however overexpression of a constitutively active mutant form of AMPK reduced sunitinib-mediated apoptosis. In intact rodents, sunitinib induced mitochondrial abnormalities and hypertrophy in cardiac myocytes (Kerkela et al., 2009). However, the use of NRVM to study consequences and causes of adult human cardiac injury may be misleading for a number of reasons including possible differences between human and rodent cardiac biology as well as energy homeostasis mechanisms (Brouillette et

al., 2004; Force and Kolaja, 2011; Gussak et al., 2000). Thus, using new, more relevant human *in vitro* models, such as stem cell derived cardiomyocytes will provide novel learning about human drug-induced injury.

Recent advances in stem cell culture have led to the directed differentiation of pluripotent cells into maturing cells that include cardiomyocytes (Kattman et al., 2011). Unlike primary culture models of human cardiomyocytes that proliferate and lose their ability to beat, human iPSC-CMs are post-mitotic, express cardiac contractile proteins, and have the entire complement of functional electrophysical channels to allow the physical contraction of the myocytes (Anson et al., 2011). Characterization of terminally differentiated iPSC-CMs revealed puntated fibrous striations of cardiac specific α/β-myosin heavy chains, cardiac troponin T, actin-related proteins; and ion channels (Na+, L-type Ca 2+, and hERG) expressed at the intermembrane surfaces (Guo et al., 2011). Moreover, successful myocyte formation of iPSC-CMs was further characterized by measuring physical contraction of the myocytes, with synchronous oscillations of 40 beats per minute, and measuring functional electrophysical properties by use of multielectrode array (Guo et al., 2011). It is reasonable to assume that these functional human cardiomyocytes might possess metabolic mechanisms that are more similar to those in the intact human heart as compared with either primary cell cultures or non-human based *in vitro* models.

In the present study, the involvement of AMPK in sunitinib-mediated cardiotoxicity in human iPSC-CMs was explored. Two known AMPK activators, AICAR and metformin (Corton et al., 1995; Towler and Hardie, 2007), were unable to attenuate substantial sunitinib-mediated toxicity. Furthermore, additional inhibitors of AMPK (RO-3857, RO-9568, RO-1652) were found to be non-cardiotoxic, which led us to reexamine the potential off-target kinase inhibition profile of sunitinib. Similar to AMPK, Ribosomal S 6 kinase (RSK) also had a dissociation constant (Kd) within the therapeutic plasma range of sunitinib (0.1 μM) and was predicted to be a critical off-target kinase mediating-sunitinib cardiotoxicity (Fabian et al., 2005; Force et al., 2007). RSK kinases carry out various cellular functions, such as involvement in proliferation, growth, motility, and survival (Anjum and Blenis, 2008). An irreversible inhibitor of RSK1/2/4 kinases did not induce cytotoxicity. This study highlights the complexity of dissecting sunitinib-mediated cardiotoxicity from adverse conduction effects, as an extensive electrophysiological analysis of sunitinib-mediated inhibition of the sodium and hERG channels and examination of field potential changes were performed. Utilization of a novel *in vitro* human cardiomyocyte model allowed for a unique analysis of sunitinib-mediated electrophysiological effects, which may shed some light on the mechanism resulting in sunitinib-mediated adverse conduction events.

Materials and methods

Chemicals

Sunitinib was purchased from LGM Pharmaceuticals (Boca Raton, FL). AICAR and metformin were purchased from Sigma Aldrich (St. Louis, MO). RO-3857, RO-9568, and RO-1652 compounds were synthesized at Roche. The RSK1/2/4 inhibitor, fluoromethylketone methoxyethylamine (RSK FMK-MEA), was synthesized by the same

procedure used to synthesize fluoromethylketone propargylamine (Cohen et al., 2007), with the exception that methoxyethylamine was used instead of propargylamine.

Cell culture

Human induced pluripotent stem cell-derived human cardiomyocytes (iCells) from Cellular Dynamics International (CDI, http://www.cellulardynamics.com/products/cardiomyocytes.html) were thawed in Plating Media (CDI) and plated as single cells onto collagen-coated 96-well plates (BD Biosciences) at a density of 50×10^3 viable-adherent cells per well (percent adherence documented on iCell data sheet). Additionally, iCells cultured for Micro-electrode Array (MEA) experimentation were thawed in Plating Media and plated onto 0.1% Gelatin (Sigma)-coated 6-well tissue-culture plates at a density of 2.2–2.7×10^6 cells per well. Cells were cultured for 5–7 days, changing the media with Maintenance Media (CDI) every two days after thawing.

Western blot analysis

iCell cardiomyocytes were lysed with Cell Lysis Buffer 1× (Cell Signaling Technology) containing 1 mM Pefabloc SC (Roche Applied Science), 1× Protease Inhibitor Tablet (Roche Applied Science), and Phosphatase Inhibitor Cocktail (Sigma Aldrich). Protein concentration was determined with the Qubit Protein Assay (Invitrogen). Protein was subjected to 10 or 12% SDS-PAGE and proteins were electrophoretically transferred to PVDF membranes (Bio-Rad trans-blot system). Membranes were blocked in ODYSSEY Blocking Buffer (LI-COR Biosciences, Lincoln, NE). Primary antibodies pACC-S79, ACC, pAMPK-T172, AMPK, and RSK1 (Cell Signaling Technologies), and GAPDH (Sigma Aldrich) were incubated, in 5% BSA in 1× TBS-0.1% Tween 20, overnight at 4 °C with gentle shaking. The secondary-immunoglobulin was conjugated with donkey-anti-mouse IR Dye 800 CW or donkey-anti-rabbit IR Dye 680 (LI-COR Biosciences) at a 1:15000 dilution. The blots were visualized Odyssey Infrared Imaging System (LI-COR Biosciences).

Cell viability assays

Following treatment of iCells for 24 h, release of lactate dehydrogenase (LDH), ATP content, Caspase 3/7 cleavage, and GSH were monitored. LDH release by damaged cells into the supernatant was determined by the Cytotoxicity Detection Kit (LDH) (Roche Applied Science). ATP present in metabolically active cells was quantified using the CellTiter-Glo Luminescent Cell Viability Assay (Promega). Cellular apoptosis was measured using the Caspase-Glo 3/7 Assay (Promega). Cellular glutathione (GSH) was measured using the GSH-Glo Glutathione Assay (Promega). All assays were performed according to manufacturer's recommendations. Signals were quantified using an Envision 2104 Multilabel Reader (Perkin Elmer) at 490 nm for LDH and luminescent signal for ATP, Caspase-3/7, and GSH.

Kinase inhibition

Sunitinib, RO-3857, RO-9568, and RO-1652 were sent to Ambit Biosciences (San Diego, CA) for kinase selectivity analysis against 227 to 353 kinases using KINOMEscan assays. In this cell free binding assay, ligand-bound kinase quantities are measured in the presence and

absence of the compound. The values reported are in terms of percent inhibition (%) for each compound against each of the kinases.

MEA experimentation

MEAs were prepared according to manufacturer guidelines. Briefly, microelectrodes in 6-well MEA dishes were coated with 2 μL Fibronectin (Sigma) diluted 1:20 and incubated at 37 °C for 3 h. iCells were reseeded at the target density of 3×10^4 cells in a 2 μL delivery to microelectrodes and incubated at 37 °C, 7% CO_2 for 3 h prior to filling each well with Maintenance Media (CDI). The media of MEAs were changed every 2 days thereafter, using Maintenance Media warmed to 37 °C. Cells were cultured for 3–7 days prior to conducting an experiment. Sunitinib stocks were prepared in DMSO at 30 mM and frozen at −80 °C until use. For MEA experimentation, sunitinib stock was serially diluted in Maintenance Media to 20× the target concentrations. MEAs were equilibrated for 15 min within the MEA60 recorder system (Multichannel Systems), prior to compound exposure. The MEA atmosphere was maintained at 37 °C, 95% O_2, and 5% CO_2 during recordings in a custom designed chamber. Compound additions were made in cumulatively increasing additions by factors of 10 to prevent disruption of electro currents, recording for 15 min at each concentration. Each 6-well MEA possessed at least one well as the time-matched vehicle (DMSO) control.

PatchXpress hERG and Nav1.5 assessment

The detailed method to quantify hERG channel inhibition by the automated patch clamp system PatchXpress® 7000A (Molecular Devices, Sunnyvale, CA) has been described elsewhere (Guo and Guthrie, 2005). In brief, Chinese hamster ovary (CHO) cells transfected with the human ether-a-go-go-related gene (hERG) was cultured in Ex-cell 302 media supplemented with 10% fetal bovine serum (FBS), 2 mM glutamine and 0.25 mg/mL geneticin and maintained in a CO_2 incubator at 37 °C. For patch clamp electrophysiology, the external buffer contained (in mM): 150 NaCl, 10 Hepes, 4 KCl, 1.2 $CaCl_2$, 1 $MgCl_2$, pH7.4 adjusted with HCl and the internal recording solution contained (in mM): 140 KCl, 6 EGTA, 5 Hepes, $MgCl_2$, 5 ATP-Na_2, pH 7.2 adjusted with KOH. Once the cell was loaded in the recording chamber and formed a giga ohm seal with the planar glass electrodes (Sealchip™), a whole-cell configuration was achieved by rupturing the cell membrane. The membrane potential was then clamped at −80 mV and the hERG channel activated by a 500 ms-depolarizing pulse delivered at 0.1 Hz, the hERG current was measured during the 500 ms-repolarizing pulse to −40 mV. For Nav1.5 channels, Chinese hamster lung cells (CHL) transfected with human Nav1.5 channel gene (SCN5A) was cultured in DMEM media supplemented with 10% FBS and 0.5 mg/mL geneticin in a CO_2 incubator at 37 °C. To measure the Nav1.5 channel current, the cells were bathed in the external buffer containing (in mM): 50 NaCl, 110 DL-aspartic acid, 1 KCl, 1 $MgCl_2$, 1.8 $CaCl_2$, 10 Hepes, 10 glucose, pH 7.4 titrated with gluconic acid, and the internal contained (in mM): 130 CsOH, 130 gluconic acid, 5 CsCl, 5 NaCl, 1 $MgCl_2$, 2 ATP-Mg, 0.2 GTP-Li, 0.5 EGTA, 10 Hepes, and pH 7.3 titrated with gluconic acid. Once the whole-cell configuration was established, the cell membrane potential was clamped at −80 mV. To activate Nav1.5 channels, the membrane was first hyperpolarized to −120 mV for 100 ms, followed by depolarization to −10 mV for 30 ms before returning to −80 mV. The testing pulses were applied at 3 Hz.

After an acceptable hERG or Nav1.5 current recording was obtained, the cell was first exposed to 0.3% DMSO as the vehicle control, followed by the test article in three ascending, full-log interval concentrations and finally E-4031 at 1 μM or tetracaine at 30 μM as the positive controls to block the hERG and Nav1.5 channel current completely. The inhibition of hERG or Nav1.5 channel current at each drug concentration was normalized to the baseline (pre-drug) level, and fitted with Hill equation to calculate IC_{50}.

Results

Sunitinib induces cardiac myocyte injury in human iPSC-CMs

The effect of sunitinib on cardiac structure, mitochondrial function, and cytotoxicity has been previously characterized in NRVM (Chu et al., 2007; Hasinoff et al., 2008; Kerkela et al., 2009), but has not been defined in human cardiac cells, either primary or stem cell-derived (Chu et al., 2007; Di Lorenzo et al., 2009). To identify the appropriate time point to examine sunitinib-mediated cardiotoxicity, we conducted a dose range-finding study with 3.9 to 250 μM sunitinib every 2 h for a 48 h time course (unpublished results). The treatment duration selected for this study was 24 h with a concentration range of 8 to 31 μM (Fig. 1). At 31 μM of sunitinib, near 100% depletion of ATP, cleavage of caspase 3/7, oxidation of GSH, and release of LDH was observed (Fig. 1). Compared to vehicle treated cells, at 23 μM of sunitinib, greater than 60% of ATP was depleted, 67% of GSH was oxidized, and a 300% increase in LDH release was observed (Fig. 1). Based on the dose–response data for ATP depletion, the TC_{50} in human iPSC-CMs was 16.7 μM for sunitinib. These cytotoxicity data suggests sunitinib treatment of human iPSC-CMs depleted ATP, induced apoptosis and oxidative stress, and led to the loss of barrier integrity of the cell membrane and established the 24 h, low μM dose curve used in subsequent studies.

Effect of AMPK over-activation on sunitinib-mediated cardiotoxicity in iPSC-CMs

AMPK is inhibited by sunitinib at a clinically relevant concentration (Deeks and Keating, 2006; Faivre et al., 2006), andmay be important in cardiac injury (Force et al., 2007; Force and Kolaja, 2011). If sunitinib did inhibit AMPK, the loss of phosphorylation on acetyl-CoA carboxylase (ACC-Ser79) by AMPK would result in enhanced ACC activity and increased consumption of ATP (Davies et al., 1990; Hardie, 2003, 2004). The inhibition of phosphorylation of AMPK's downstream target, ACC-Ser79, was measured to confirm that sunitinib (15 μM for 2 h) inhibited AMPK in human iPSC-CMs (Fig. 2A).

To determine if AMPK activation could attenuate sunitinib cardio-toxicity, human iPSC-CMs were pretreated for 3 h with 1 or 2 mM AICAR or metformin. Western blot analysis of the phosphorylation status of AMPKα-Thr172 and its downstream target ACC-Ser79 confirmed both AICAR and metformin treatment activated AMPK signaling in iPSC-CMs (Fig. 2B). Following a 3 h pretreatment of 1 or 2 mM AICAR or metformin, iPSC-CMs were treated for 24 h with a single dose of 8 to 31 μM of sunitinib. Neither AICAR (Fig. 3A) nor metformin (Fig. 3E) attenuated sunitinib-mediated ATP depletion. Pretreatment with 1 mM AICAR of 31 μM sunitinib resulted in a 14% attenuation of oxidized GSH (Fig. 3B, $p < 0.001$). Additionally, maximal attenuation of caspase 3/7 cleavage of 108% was observed with 2 mM AICAR pretreatment of 23 μM sunitinib (Fig. 3C, $p < 0.01$), and an 80%

reduction of LDH release with 1 mM AICAR pretreatment of 23 or 31 μM sunitinib (Fig. 3D, $p < 0.001$). Similarly, a 35% reduction in oxidation of GSH was observed with 2 mM metformin pretreatment of 23 μM sunitinib (Fig. 3F, $p < 0.01$). Maximal attenuation of caspase 3/7 cleavage of 107% (Fig. 3G, $p < 0.01$) and LDH release of 90% (Fig. 3H, $p < 0.01$) was observed with 1 mM metformin pretreatment of 23 μM sunitinib. Since neither AMPK activator attenuated ATP depletion, these data suggest AMPK is not critical inmediating sunitinib-mediated cardiotoxicity in human iPSC-CMs.

AMPK kinase inhibitors are not cardiotoxic in iPSC-CMs

To further evaluate the role of AMPK in cytotoxicity, internally developed small molecule kinase inhibitors of AMPKα1/α2 (RO-3857, RO-9568, RO-1652) were tested in human iPSC-CMs. AMPKα1/α2 are inhibited in a range 93–98% binding (See Supplemental Figs. 2–4, respectively, for the kinase inhibition profiles and compound structure). The downstream signaling of AMPK was investigated for RO3857; treatment with 31 μM AMPK inhibitor (RO-3857) and 15.6 μM sunitinib both decreased the phosphorylation status of ACC-S79 (Fig. 4, lanes 2–3). GAPDH protein expression was not changed in any of the treatment conditions, indicating no effects on viability occurred during the treatments (Fig. 4).

A dose response curve was generated in iPSC-CMs treated with 4 to 250 μM AMPK inhibitors. The AMPK inhibitors, RO-3857 and RO-9568, did not change ATP or LDH at any concentration tested (Figs. 5A and B), whereas RO-1652 resulted in cytotoxicity only at the highest concentration of 250 μM (Fig. 5C). These data suggest that inhibition of AMPK does not result in cytotoxicity and that AMPK is most likely not involved in sunitinib-mediated cardiotoxicity.

RSK1/2/4 inhibition does not mediate sunitinib cardiotoxicity in human iPSC-CMs

Ribosomal S 6 kinase (RSK) was identified as a potential target of sunitinib (Fabian et al., 2005). Sunitinib inhibited RSK1 and RSK2 with K_d values of 0.14 μM and 0.017 μM, respectively (Karaman et al., 2008). Furthermore, in a kinase activity assay, sunitinib inhibited RSK1 with an IC_{50} value of 0.36 μM (Hasinoff et al., 2008), which is within the therapeutic plasma concentration range of 0.1 μM for sunitinib (Faivre et al., 2007). In the 10 μM AMBIT screen (Supplemental Fig. 1) RSK1/2/4 were potently inhibited at 100% by sunitinib. The protein expression of RSK1 in human iPSC-CMs was confirmed by Western blot (Fig. 6A). Therefore, RSK1/2/4 may be critical targets mediating sunitinib cardiotoxicity.

To evaluate the role of RSK in cardiotoxicity, a dose response curve was generated in iPSC-CMs treated with 4 to 250 μM of RSK FMK-MEA, an irreversible inhibitor of RSK1/2/4 kinases (Cohen et al., 2005). Treatment with up to 62 μM of the RSK1/2/4 inhibitor did not result in ATP depletion or LDH release (Fig. 6A). Based on the dose–response data for ATP depletion, the TC_{50} of RSK FMK-MEA in human iPSC-CMs is 250 μM (Fig. 6). Therefore, sunitinib cardiotoxicity does not appear to be mediated through off-target RSK inhibition.

Sunitinib and the RSK inhibitor mediate contractile and electrophysiological changes in human iPSC-CMs

In patients, cardiac adverse events associated with sunitinib treatment are hypertension, reductions in left ventricular ejection fraction (LVEF), and congestive heart failure (Chu et al., 2007; Di Lorenzo et al., 2009; Faivre et al., 2007; Telli et al., 2008). The decrease in LVEF has been postulated to be a direct result of cardiomyocyte injury (Chu et al., 2007). Another effect of sunitinib, observed in patients, is a dose-dependent delay in cardiac repolarization resulting in prolongation of the QT interval (Bello et al., 2009). To detect sunitinib mediated changes in cardiac electrophysiology, in synchronously beating human iPSC-CMs, microelectrode arrays were used (MEA). Recordings on MEA were made for 15 min at each concentration and a dose-dependent reduction in beat rate was observed at concentrations as low as 1 μM sunitinib (Figs. 7A–B). This was accompanied by the prolongation of fPDc (field-potential duration corrected by the beat rate with Fridericia formula) (Fig. 7B), a parameter resembling action potential duration in a single cardiomyocyte or QT interval in a heart. Furthermore, sunitinib dose-dependently reduced the amplitude of the Na^+-peak, and Ca^{2+}-waveform at higher concentrations in iPSC-CMs, suggestive of altered Na^+ and Ca^{2+} cycling. At 10 μM sunitinib, MEA field potential traces depicted intermittent small, irregular (arrhythmic) beats with altered amplitude and beat duration at 30 μM sunitinib (Fig. 7B). These observations of sodium peak reduction and the initiation of these irregular arrhythmic beats, reminiscent of the field potential changes due to specific hERG channel blockers, prompted the examination of the effects of sunitinib and the RSK1/2/4 inhibitor by whole cell, single channel patch clamp analysis. To determine the effect of sunitinib on the potassium permeable, voltage-gated ion channel hERG, which mediates the repolarizing I_{Kr} current of the cardiac action potential, and the effect of sunitinib on the voltage-gated human heart sodium channel (Nav1.5), PatchXpress with Chinese hamster ovary (CHO) cells expressing the human ether-a-go-go-related gene (hERG) and Chinese hamster Lung (CHL) cells expressing Nav1.5, respectively was used. Based on a dose–response curve with sunitinib in CHO-hERG cells, the IC_{50} value of hERG inhibition is 1.4 μM, and the IC_{50} value of Nav1.5 channel inhibition is 7.0 μM (Fig. 7C).

While the deleterious electrophysiological effects of sunitinib are likely mediated by simultaneous hERG and Nav1.5 blockade, the role of off-target kinase inhibition on conduction effects was explored by modulating RSK and AMPK kinases. Treatment with the highly selective, irreversible RSK1/2/4 inhibitor (Cohen et al., 2007) resulted in a dose-dependent reduction in the amplitude of the Na^+-peak, and distinct irregular (arrhythmic) beats with altered amplitude and beat duration as low as 3 μM RSK FMK-MEA which was accompanied by the dose-dependent prolongation of fPDc (Figs. 7D–E). To determine the effect of the RSK inhibitor on hERG and Nav1.5 channels in CHO-hERG and CHL-Nav1.5 cells respectively, we utilized PatchXpress. Based on a dose–response curve with RSK FMK-MEA, the IC_{50} value of hERG inhibition is 2.2 μM, and the IC_{50} value of Nav1.5 channel inhibition is 56.8 μM (Fig. 7F).

Given that activating mutations in the γ2 subunit of AMPK, observed in Wolfe–Parkinson–White (WPW) patients, is associated with ventricular pre-excitation and atrial tachyarrythmias (Ahmad et al., 2005; Arad et al., 2003; Blair et al., 2001; Dyck and

Lopaschuk, 2006; Oliveira et al., 2003; Zhang et al., 2008), the perturbation (overactivation or inhibition) of AMPK activity may result in conduction effects. Stimulation of AMPK with up to 2 mM of AICAR or metformin did not significantly change the beat rate (up or down) greater than 1% from baseline (Figs. 8A–B). Inhibition of AMPK with both RO-9568 and RO-3857 resulted in a clear decrease in amplitude and increase in beat rate with 30 to 60 μM treatments (Figs. 8C–D). The increased beat rate may be attributed to blocking the calcium peak; a result similar to the increase in beat rate seen with the L-type Ca^{2+} channel blocker nifedipine (Shen et al., 2000).

Discussion

Derivation of human iPSC-CMs with functional sarcomeric structures and channel activity enabled mechanistic assessment of the toxicity of sunitinib. Previously, human drug-induced toxicity research was limited to extrapolations from animal models that may not properly predict human response, primary tissues which suffer from dedifferentiation and donor-to-donor variability, or transformed cell lines that bear little resemblance to their tissue-of-origin (Bistola et al., 2008; Davidson et al., 2005; Field, 1988; Force and Kolaja, 2011; Gussak et al., 2000; Kimes and Brandt, 1976; Simpson and Savion, 1982; White et al., 2004; Zhang et al., 2009). Human iPSC-CMs are an improvement given their resemblance to intact tissues on a genomic, transcriptional, and functional nature.

Human iPSC-CMs were used to investigate the involvement of AMPK and RSK in sunitinib-mediated cardiotoxicity. The potent inhibition of hERG by the RSK1/2/4 inhibitor confounds the interpretation of the electrophysiology data (MEA) and the role inhibition of RSK may play in sunitinib-mediated arrhythmias. Studies published by Kerkela et al. (2009) reported that overexpression of a constitutively active AMPK mutant in NRVMs reduced sunitinib-mediated apoptosis. Conversely, our studies are in agreement with Hasinoff et al. (2008) who reported that pretreatment with metformin failed to attenuate sunitinib cardiotoxicity (LDH release) in NRVMs. Both Kerkela and Hasinoff employ the TUNEL assay or LDH release to analyze sunitinib cardiotoxicity, which may not be as predictive as myocyte ATP content. During metabolic stress, AMPK maintains energy homoestasis by increasing ATP generation and regulating glucose and fatty acid metabolism (Dyck and Lopaschuk, 2006). Vast amounts of ATP are necessary to mediate the contractile activity of sarcomeres, and when ATP generation is perturbed, the minimal cardiac ATP reserves are depleted within seconds (Dyck and Lopaschuk, 2006; Force and Kolaja, 2011; Khouri et al., 1965). Therefore, measuring mitochondrial ATP is an excellent gage of the cardiomyocytes ability to function, as well as survive. In human iPSC-CMs, we observed a rapid depletion of ATP (80%) by 4.5 h, and as early at 1.7 h a significant increase in apoptosis and GSH oxidation with 31 μM sunitinib (unpublished results). In human iPSC-CMs treated with sunitinib, ATP was dose-dependently depleted by 24 h, and a parallel increase in apoptosis, GSH oxidation, and LDH release was also observed. An explanation of why attenuation of apoptosis, and not ATP depletion, was observed; is that studies in the heart suggest that AMPK activation is antiapoptotic (Hickson-Bick et al., 2000; Russell et al., 2004; Shibata et al., 2005; Terai et al., 2005; Dyck and Lopaschuk, 2006; Spector et al., 2007). In particular, Shibata et al. (2005) demonstrated that adiponectin induced AMPK activation attenuated apoptosis in hypoxia-induced NRVMs. It is thought that energy depletion is a critical trigger

of apoptosis (Dyck and Lopaschuk, 2006), therefore, the attenuation of caspase 3/7 cleavage following overactivaton of AMPK should have resulted in a parallel rescue of ATP. Therefore, the inability of AMPK activation to overcome sunitinib-mediated ATP depletion, combined with the lack of cardiotoxicity of small molecule inhibitors of AMPK, strongly suggests that AMPK alone is not a critical protein contributing to the cytotoxicity of sunitinib.

Although the cytotoxicity of sunitinib is likely unrelated to the conduction effects, conduction abnormalities could lead to ischemic injury in the heart that may cause direct tissue damage (Topol, 2007). Changes in the electrical current have been reported to lead to conduction effects which caused valve injury in patients (Topol, 2007). Therefore, it is important to investigate changes in conduction and electrophysiological properties following treatment with sunitinib and SMIs in human iPSC-CMs, which have synchronous oscillations in a monolayer (Guo et al., 2011). Sunitinib-induced electrophysiological changes including decreased sodium and calcium peaks and a decrease in the beat rate/duration that were detected with as low as 1 μM sunitinib. To further explore sunitinib inhibition of critical cardiac channels, the direct inhibition of hERG and Nav1.5 channels was measured by automated patch clamp. The change in the depolarization observed *in vitro* in iPSC-CMs, confirmed by Nav1.5 channel inhibition (Nav1.5 IC_{50} Fig. 7), parallels the sunitinib-mediated changes in cardiac repolarization and prolongation of the QT interval seen in the clinic (Bello et al., 2009). Altered depolarization of the ventricles suggest a change in the flow between RV and LV, and may predispose the myocardium to damage; which may relate to decreases in LVEF seen in the clinic following sunitinib treatment (Chu et al., 2007).

The inhibition of AMPK could be a plausible explanation for the decrease in amplitude and beat rate that results from sunitinib treatment, given that Wolfe-Parkinson-White (WPW) syndrome patients with overactivation of AMPK experience ventricular pre-excitation and atrial tachyarrythmias (Dyck and Lopaschuk, 2006). Patients with WPW syndrome have mutations in AMPKγ2 that lead to higher basal activity of cardiac AMPKα, insensitivity to increases in AMP, increased cardiac glycogen, and profound cardiac hypertrophy (Dyck and Lopaschuk, 2006). Although the use of potent AMPK inhibitors resulted in a decrease in amplitude, the beat rate was increased, which was the opposite effect seen with sunitinib treatment. The increased beat rate may be attributed to off-target inhibition of kinases other than AMPK, such as calcium-calmodulin-dependent protein kinases (CAMK1, CAMK1D, CAMKK2, CAMK2D, and CAMK2A) which have been inhibited to varying degrees by the AMPK inhibitors and have been implicated in regulating heart beat (Maier and Bers, 2002).

To interrogate the list of prospective off-target kinases that may be involved in mediating sunitinib cardiotoxicity, we compared kinases that were inhibited (Supplemental Fig. 1) to a known list of kinases of importance in the heart (Force and Kolaja, 2011) (Table 1A). Of 50 kinases relevant to the heart, 18 of those kinases were inhibited less than 50% by sunitinib (Table 1A), and another 14 of those kinases were inhibited by the AMPK inhibitors (RO-3857, RO-9568, and RO-1652) that were not cardiotoxic (Table 1B). The simplified list of 13 kinases that may be involved in sunitinib-mediated cardiotoxicity are highlighted (pink) (Table 1A). A number of studies geared towards profiling FDA approved cardiotoxic

TKIs, including sunitinib, correlated cardiac myocyte damage with lack of target specificity (Hasinoff, 2010; Hasinoff and Patel, 2010). Therefore, sunitinib cardiotoxicitymay not be attributed to off-target inhibition of a single kinase, but a synergistic effect compounded by inhibition of multiple kinases.

The availability of appropriate models for use during the drug development process is critical to predicting adverse cardiac events and reducing pre-clinical drug attrition rates. This lack of relevant predictive models has made it difficult to generate biologically meaningful cardiotoxicity data. Therefore, utilization of human iPSC-CMs to perform mechanistic studies (electrophysiological, contractile, and signal transduction) which were not previously possible, may allow for a method to screen earlier for cardiac dysfunction. Human iPSC-CMs are a novel model for the detection of drug-induced cardiotoxicity, and may be a better predictive model to address adverse cardiac events preceding the clinical stages of development of a compound.

Supplementary Material

Refer to Web version on PubMed Central for supplementary material.

Acknowledgments

Conflict of interest statement

Fluoromethylketone RSK inhibitors are described in patent applications filed by the University of California, on which J.T. is a co-inventor. Part of this work was supported by the National Institutes of Health [GM071434 to J.T.].

The authors would like to acknowledge Thomas Singer, Andreas Strauss and Thomas Weiser for their managerial support of this project.

Abbreviations

AMPK	AMP-activated protein kinase
RSK	ribosomal S 6 kinase
iPSC-CMs	induced pluripotent stem cell-derived human cardiomyocytes
TKIs	tyrosine kinase inhibitors
NRVM	neonatal rat ventricular myocytes
LDH	lactate dehydrogenase
AICAR	aminoimidazole carboxamide ribonucleotide
GSH	glutathione
ACC-Ser79	acetyl-CoA carboxylase
HEK293	Human embryonic kidney cells
FMK-MEA	RSK-fluoromethylketone-methoxyethylamine

References

Ahmad F, Arad M, Musi N, He H, Wolf C, Branco D, Perez-Atayde AR, Stapleton D, Bali D, Xing Y, Tian R, Goodyear LJ, Berul CI, Ingwall JS, Seidman CE, Seidman JG. Increased alpha2 subunit-associated AMPK activity and PRKAG2 cardiomyopathy. Circulation. 2005; 112:3140–3148. [PubMed: 16275868]

Anjum R, Blenis J. The RSK family of kinases: emerging roles in cellular signalling. Nat. Rev. Mol. Cell. Biol. 2008; 9:747–758. [PubMed: 18813292]

Anson BD, Kolaja KL, Kamp TJ. Opportunities for use of human iPS cells in predictive toxicology. Clin. Pharmacol. Ther. 2011; 89:754–758. [PubMed: 21430658]

Arad M, Moskowitz IP, Patel VV, Ahmad F, Perez-Atayde AR, Sawyer DB, Walter M, Li GH, Burgon PG, Maguire CT, Stapleton D, Schmitt JP, Guo XX, Pizard A, Kupershmidt S, Roden DM, Berul CI, Seidman CE, Seidman JG. Transgenic mice overexpressing mutant PRKAG2 define the cause of Wolff–Parkinson–White syndrome in glycogen storage cardiomyopathy. Circulation. 2003; 107:2850–2856. [PubMed: 12782567]

Bantscheff M, Eberhard D, Abraham Y, Bastuck S, Boesche M, Hobson S, Mathieson T, Perrin J, Raida M, Rau C, Reader V, Sweetman G, Bauer A, Bouwmeester T, Hopf C, Kruse U, Neubauer G, Ramsden N, Rick J, Kuster B, Drewes G. Quantitative chemical proteomics reveals mechanisms of action of clinical ABL kinase inhibitors. Nat. Biotechnol. 2007; 25:1035–1044. [PubMed: 17721511]

Bello CL, Mulay M, Huang X, Patyna S, Dinolfo M, Levine S, Van Vugt A, Toh M, Baum C, Rosen L. Electrocardiographic characterization of the QTc interval in patients with advanced solid tumors: pharmacokinetic–pharmacodynamic evaluation of sunitinib. Clin. Cancer. Res. 2009; 15:7045–7052. [PubMed: 19903787]

Bistola V, Nikolopoulou M, Derventzi A, Kataki A, Sfyras N, Nikou N, Toutouza M, Toutouzas P, Stefanadis C, Konstadoulakis MM. Long-term primary cultures of human adult atrial cardiac myocytes: cell viability, structural properties and BNP secretion in vitro. Int. J. Cardiol. 2008; 131:113–122. [PubMed: 18255169]

Blair E, Redwood C, Ashrafian H, Oliveira M, Broxholme J, Kerr B, Salmon A, Ostman-Smith I, Watkins H. Mutations in the gamma(2) subunit of AMP-activated protein kinase cause familial hypertrophic cardiomyopathy: evidence for the central role of energy compromise in disease pathogenesis. Hum. Mol. Genet. 2001; 10:1215–1220. [PubMed: 11371514]

Brouillette J, Clark RB, Giles WR, Fiset C. Functional properties of K + currents in adult mouse ventricular myocytes. J. Physiol. 2004; 559:777–798. [PubMed: 15272047]

Chu TF, Rupnick MA, Kerkela R, Dallabrida SM, Zurakowski D, Nguyen L, Woulfe K, Pravda E, Cassiola F, Desai J, George S, Morgan JA, Harris DM, Ismail NS, Chen JH, Schoen FJ, Van den Abbeele AD, Demetri GD, Force T, Chen MH. Cardiotoxicity associated with tyrosine kinase inhibitor sunitinib. Lancet. 2007; 370:2011–2019. [PubMed: 18083403]

Cohen MS, Zhang C, Shokat KM, Taunton J. Structural bioinformatics-based design of selective, irreversible kinase inhibitors. Science. 2005; 308:1318–1321. [PubMed: 15919995]

Cohen MS, Hadjivassiliou H, Taunton J. A clickable inhibitor reveals context-dependent autoactivation of p90 RSK. Nat. Chem. Biol. 2007; 3:156–160. [PubMed: 17259979]

Corton JM, Gillespie JG, Hawley SA, Hardie DG. 5-aminoimidazole-4-carboxamide ribonucleoside. A specific method for activating AMP-activated protein kinase in intact cells? Eur. J. Biochem. 1995; 229:558–565. [PubMed: 7744080]

Davidson MM, Nesti C, Palenzuela L, Walker WF, Hernandez E, Protas L, Hirano M, Isaac ND. Novel cell lines derived from adult human ventricular cardiomyocytes. J. Mol. Cell. Cardiol. 2005; 39:133–147. [PubMed: 15913645]

Davies SP, Sim AT, Hardie DG. Location and function of three sites phosphorylated on rat acetyl-CoA carboxylase by the AMP-activated protein kinase. Eur. J. Biochem. 1990; 187:183–190. [PubMed: 1967580]

Deeks ED, Keating GM. Sunitinib. Drugs. 2006; 66:2255–2266. discussion 2267–2258. [PubMed: 17137406]

Di Lorenzo G, Autorino R, Bruni G, Carteni G, Ricevuto E, Tudini M, Ficorella C, Romano C, Aieta M, Giordano A, Giuliano M, Gonnella A, De Nunzio C, Rizzo M, Montesarchio V, Ewer M, De Placido S. Cardiovascular toxicity following sunitinib therapy in metastatic renal cell carcinoma: a multicenter analysis. Ann. Oncol. 2009; 20:1535–1542. [PubMed: 19474115]

Dyck JR, Lopaschuk GD. AMPK alterations in cardiac physiology and pathology: enemy or ally? J. Physiol. 2006; 574:95–112. [PubMed: 16690706]

Fabian MA, Biggs WH III, Treiber DK, Atteridge CE, Azimioara MD, Benedetti MG, Carter TA, Ciceri P, Edeen PT, Floyd M, Ford JM, Galvin M, Gerlach JL, Grotzfeld RM, Herrgard S, Insko DE, Insko MA, Lai AG, Lelias JM, Mehta SA, Milanov ZV, Velasco AM, Wodicka LM, Patel HK, Zarrinkar PP, Lockhart DJ. A small molecule-kinase interaction map for clinical kinase inhibitors. Nat. Biotechnol. 2005; 23:329–336. [PubMed: 15711537]

Faivre S, Delbaldo C, Vera K, Robert C, Lozahic S, Lassau N, Bello C, Deprimo S, Brega N, Massimini G, Armand JP, Scigalla P, Raymond E. Safety, pharmacokinetic, and antitumor activity of SU11248, a novel oral multitarget tyrosine kinase inhibitor, in patients with cancer. J. Clin. Oncol. 2006; 24:25–35. [PubMed: 16314617]

Faivre S, Demetri G, Sargent W, Raymond E. Molecular basis for sunitinib efficacy and future clinical development. Nat. Rev. 2007; 6:734–745.

Field LJ. Atrial natriuretic factor-SV40 T antigen transgenes produce tumors and cardiac arrhythmias in mice. Science. 1988; 239:1029–1033. [PubMed: 2964082]

Force T, Kolaja KL. Cardiotoxicity of kinase inhibitors: the prediction and translation of preclinical models to clinical outcomes. Nat. Rev. 2011; 10:111–126.

Force T, Krause DS, Van Etten RA. Molecular mechanisms of cardiotoxicity of tyrosine kinase inhibition. Nat. Rev. Cancer. 2007; 7:332–344. [PubMed: 17457301]

Guo L, Guthrie H. Automated electrophysiology in the preclinical evaluation of drugs for potential QT prolongation. J. Pharmacol. Toxicol. Methods. 2005; 52:123–135. [PubMed: 15936217]

Guo L, Abrams RM, Babiarz JE, Cohen JD, Kameoka S, Sanders MJ, Chiao E, Kolaja KL. Estimating the risk of drug-induced proarrhythmia using human induced pluripotent stem cell-derived cardiomyocytes. Toxicol. Sci. 2011; 123:281–289. [PubMed: 21693436]

Gussak I, Chaitman BR, Kopecky SL, Nerbonne JM. Rapid ventricular repolarization in rodents: electrocardiographic manifestations, molecular mechanisms, and clinical insights. J. Electrocardiol. 2000; 33:159–170. [PubMed: 10819409]

Hardie DG. Minireview: the AMP-activated protein kinase cascade: the key sensor of cellular energy status. Endocrinology. 2003; 144:5179–5183. [PubMed: 12960015]

Hardie DG. The AMP-activated protein kinase pathway—new players upstream and downstream. J. Cell. Sci. 2004; 117:5479–5487. [PubMed: 15509864]

Hasinoff BB. The cardiotoxicity and myocyte damage caused by small molecule anticancer tyrosine kinase inhibitors is correlated with lack of target specificity. Toxicol. Appl. Pharmacol. 2010; 244:190–195. [PubMed: 20045709]

Hasinoff BB, Patel D. The lack of target specificity of small molecule anticancer kinase inhibitors is correlated with their ability to damage myocytes in vitro. Toxicol. Appl. Pharmacol. 2010; 249:132–139. [PubMed: 20832415]

Hasinoff BB, Patel D, O'Hara KA. Mechanisms of myocyte cytotoxicity induced by the multiple receptor tyrosine kinase inhibitor sunitinib. Mol. Pharmacol. 2008; 74:1722–1728. [PubMed: 18815214]

Hickson-Bick DL, Buja LM, McMillin JB. Palmitate-mediated alterations in the fatty acid metabolism of rat neonatal cardiac myocytes. J. Mol. Cell. Cardiol. 2000; 32:511–519. [PubMed: 10731449]

Karaman MW, Herrgard S, Treiber DK, Gallant P, Atteridge CE, Campbell BT, Chan KW, Ciceri P, Davis MI, Edeen PT, Faraoni R, Floyd M, Hunt JP, Lockhart DJ, Milanov ZV, Morrison MJ, Pallares G, Patel HK, Pritchard S, Wodicka LM, Zarrinkar PP. A quantitative analysis of kinase inhibitor selectivity. Nat. Biotechnol. 2008; 26:127–132. [PubMed: 18183025]

Kattman SJ, Koonce CH, Swanson BJ, Anson BD. Stem cells and their derivatives: a renaissance in cardiovascular translational research. J. Cardiovasc. Transl. Res. 2011; 4:66–72. [PubMed: 21061105]

Kerkela R, Woulfe KC, Durand JB, Vagnozzi R, Kramer D, Chu TF, Beahm C, Chen MH, Force T. Sunitinib-induced cardiotoxicity is mediated by off-target inhibition of AMP-activated protein kinase. Clin. Trans. Sci. 2009; 2:15–25.

Khouri EM, Gregg DE, Rayford CR. Effect of exercise on cardiac output, left coronary flow and myocardial metabolism in the unanesthetized dog. Circ. Res. 1965; 17:427–437. [PubMed: 5843879]

Kimes BW, Brandt BL. Properties of a clonal muscle cell line from rat heart. Exp. Cell. Res. 1976; 98:367–381. [PubMed: 943302]

Kudo N, Barr AJ, Barr RL, Desai S, Lopaschuk GD. High rates of fatty acid oxidation during reperfusion of ischemic hearts are associated with a decrease in malonyl-CoA levels due to an increase in 5′-AMP-activated protein kinase inhibition of acetyl-CoA carboxylase. J. Biol. Chem. 1995; 270:17513–17520. [PubMed: 7615556]

Kudo N, Gillespie JG, Kung L, Witters LA, Schulz R, Clanachan AS, Lopaschuk GD. Characterization of 5′AMP-activated protein kinase activity in the heart and its role in inhibiting acetyl-CoA carboxylase during reperfusion following ischemia. Biochim. Biophys. Acta. 1996; 1301:67–75. [PubMed: 8652652]

Maier LS, Bers DM. Calcium, calmodulin, and calcium–calmodulin kinase II: heartbeat to heartbeat and beyond. J. Mol. Cell. Cardiol. 2002; 34:919–939. [PubMed: 12234763]

Meissner K, Heydrich B, Jedlitschky G, Meyer Zu Schwabedissen H, Mosyagin I, Dazert P, Eckel L, Vogelgesang S, Warzok RW, Bohm M, Lehmann C, Wendt M, Cascorbi I, Kroemer HK. The ATP-binding cassette transporter ABCG2 (BCRP), a marker for side population stem cells, is expressed in human heart. J. Histochem. Cytochem. 2006; 54:215–221. [PubMed: 16116030]

Menna P, Salvatorelli E, Minotti G. Cardiotoxicity of antitumor drugs. Chem. Res. Toxicol. 2008; 21:978–989. [PubMed: 18376852]

Motzer RJ, Hutson TE, Tomczak P, Michaelson MD, Bukowski RM, Rixe O, Oudard S, Negrier S, Szczylik C, Kim ST, Chen I, Bycott PW, Baum CM, Figlin RA. Sunitinib versus interferon alfa in metastatic renal-cell carcinoma. N. Engl. J. Med. 2007; 356:115–124. [PubMed: 17215529]

Oliveira SM, Ehtisham J, Redwood CS, Ostman-Smith I, Blair EM, Watkins H. Mutation analysis of AMP-activated protein kinase subunits in inherited cardiomyopathies: implications for kinase function and disease pathogenesis. J. Mol. Cell. Cardiol. 2003; 35:1251–1255. [PubMed: 14519435]

Orphanos GS, Ioannidis GN, Ardavanis AG. Cardiotoxicity induced by tyrosine kinase inhibitors. Acta. Oncol. 2009; 48:964–970. [PubMed: 19734999]

Russell RR 3rd, Li J, Coven DL, Pypaert M, Zechner C, Palmeri M, Giordano FJ, Mu J, Birnbaum MJ, Young LH. AMP-activated protein kinase mediates ischemic glucose uptake and prevents postischemic cardiac dysfunction, apoptosis, and injury. J. Clin. Invest. 2004; 114:495–503. [PubMed: 15314686]

Shen JB, Jiang B, Pappano AJ. Comparison of L-type calcium channel blockade by nifedipine and/or cadmium in guinea pig ventricular myocytes. J. Pharmacol. Exp. Ther. 2000; 294:562–570. [PubMed: 10900233]

Shibata R, Sato K, Pimentel DR, Takemura Y, Kihara S, Ohashi K, Funahashi T, Ouchi N, Walsh K. Adiponectin protects against myocardial ischemia-reperfusion injury through AMPK- and COX-2-dependent mechanisms. Nat. Med. 2005; 11:1096–1103. [PubMed: 16155579]

Simpson P, Savion S. Differentiation of rat myocytes in single cell cultures with and without proliferating nonmyocardial cells. Cross-striations, ultrastructure, and chronotropic response to isoproterenol. Circ. Res. 1982; 50:101–116. [PubMed: 7053872]

Spector NL, Yarden Y, Smith B, Lyass L, Trusk P, Pry K, Hill JE, Xia W, Seger R, Bacus SS. Activation of AMP-activated protein kinase by human EGF receptor 2/EGF receptor tyrosine kinase inhibitor protects cardiac cells. Proc. Natl. Acad. Sci. USA. 2007; 104:10607–10612. [PubMed: 17556544]

Telli ML, Witteles RM, Fisher GA, Srinivas S. Cardiotoxicity associated with the cancer therapeutic agent sunitinib malate. Ann. Oncol. 2008; 19:1613–1618. [PubMed: 18436521]

Terai K, Hiramoto Y, Masaki M, Sugiyama S, Kuroda T, Hori M, Kawase I, Hirota H. AMP-activated protein kinase protects cardiomyocytes against hypoxic injury through attenuation of endoplasmic reticulum stress. Mol. Cell. Biol. 2005; 25:9554–9575. [PubMed: 16227605]

Topol, EJ. Cariac Trauma. In: Califf, Robert M.Thomas, James D., Thompson, Paul D., editors. Textbook of Cardiovascular Medicine. Lippincott Williams & Wilkins; Philadelphia: 2007.

Towler MC, Hardie DG. AMP-activated protein kinase in metabolic control and insulin signaling. Circ. Res. 2007; 100:328–341. [PubMed: 17307971]

White SM, Constantin PE, Claycomb WC. Cardiac physiology at the cellular level: use of cultured HL-1 cardiomyocytes for studies of cardiac muscle cell structure and function. Am. J. Physiol. Heart. Circ. Physiol. 2004; 286:H823–H829. [PubMed: 14766671]

Zhang P, Hu X, Xu X, Fassett J, Zhu G, Viollet B, Xu W, Wiczer B, Bernlohr DA, Bache RJ, Chen Y. AMP activated protein kinase-alpha2 deficiency exacerbates pressure-overload-induced left ventricular hypertrophy and dysfunction in mice. Hypertension. 2008; 52:918–924. [PubMed: 18838626]

Zhang Y, Nuglozeh E, Toure F, Schmidt AM, Vunjak-Novakovic G. Controllable expansion of primary cardiomyocytes by reversible immortalization. Hum. Gene. Ther. 2009; 20:1687–1696. [PubMed: 19708763]

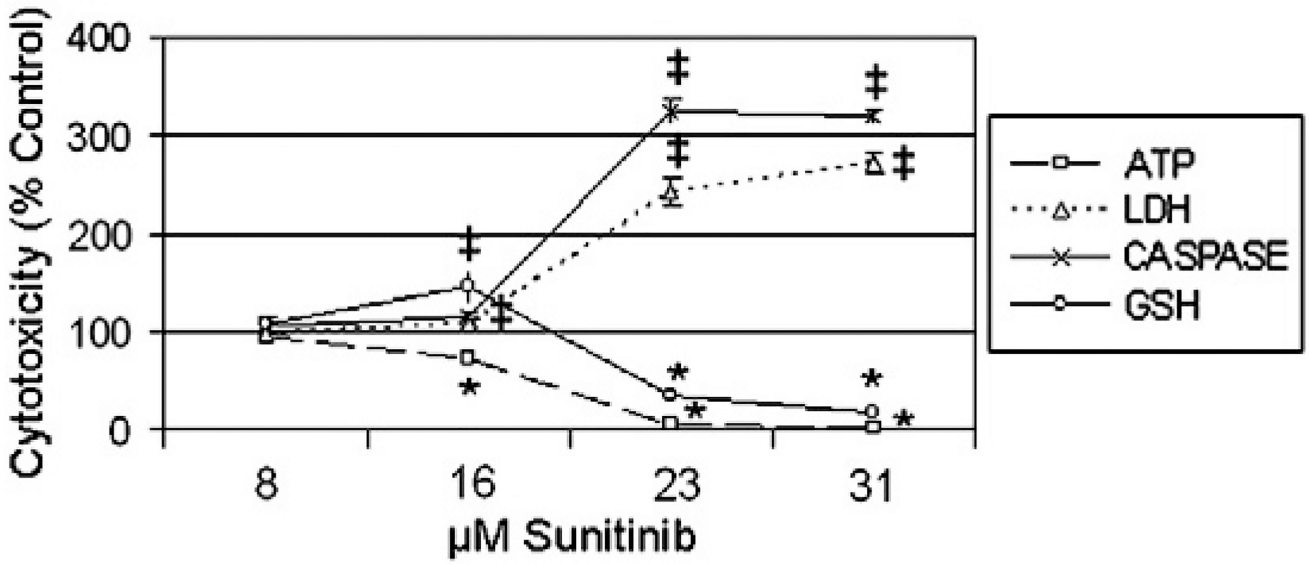

Fig. 1.

Sunitinib cardiotoxicity profile in human iPSC-CMs. iCell cardiomyocytes were treatedwith 8 to 31 μM sunitinib for 24 h; followed by ATP depletion, LDH release, caspase 3/7 cleavage, and GSH oxidation assays. N=3 for all treatment groups, and symbols denote statistically significant decrease (*) or increase (‡) between vehicle and sunitinib treatment groups, student *T*-test $p < 0.05$.

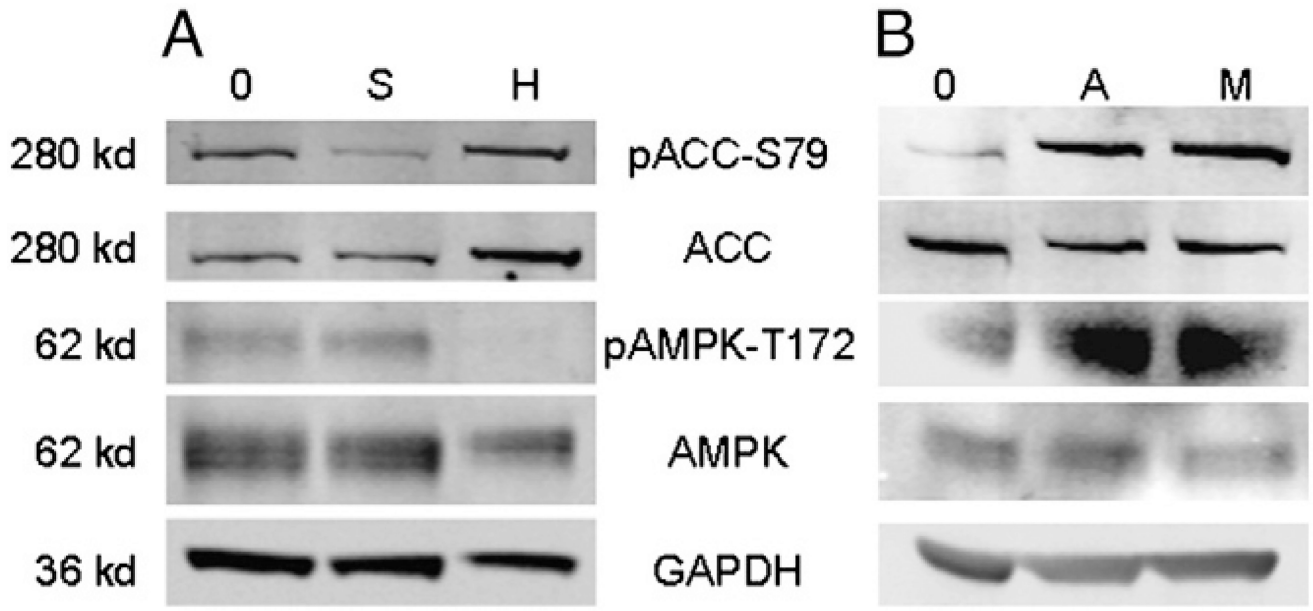

Fig. 2.

AMPK and ACC signaling inhibited by sunitinib, but activated by aminoimidazole carboxamide ribonucleotide (AICAR) or metformin treatments in iPSC-CMs. iCell cardiomyocytes were treated with (A) 15 μM sunitinib [S] for 2 h, (B) 1 mM AICAR [A] or metformin [M], or vehicle [0] for 3 h. iCell and HEK293 [H] (positive control) whole cell lysates were subjected to Western blotting with antibodies specific to pACC-S79, ACC, p-AMPK-T172, AMPK, and GAPDH.

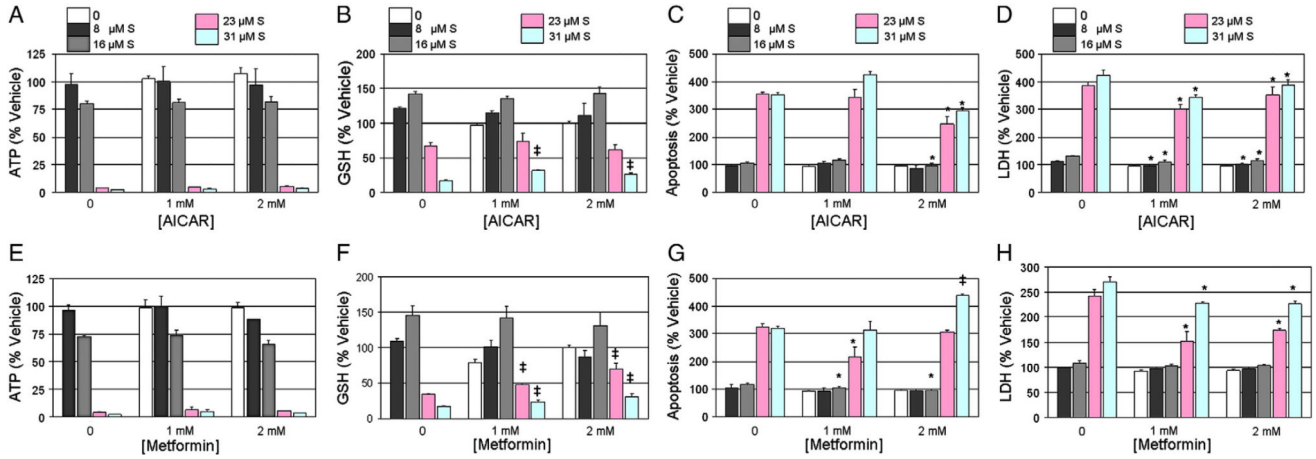

Fig. 3.

AICAR or metformin pretreatment results in marginal attenuation of sunitinib cardiotoxicity in iPSC-CMs. iCell cardiomyocytes were pretreated with 1 or 2 mM AICAR (A–D) or metformin (E–H) for 3 h, followed by treatment with 8 to 31 μM sunitinib (S) for 24 h. iCells were then assayed for (A, E) ATP depletion, (B, F) GSH oxidation, (C, G), caspase 3/7 cleavage, and, (*D, H*) LDH release. N=3 for all treatment groups, and symbols denote statistically significant decrease (*) or increase (‡) between sunitinib alone and pretreatment groups, student *T*-test $p < 0.05$.

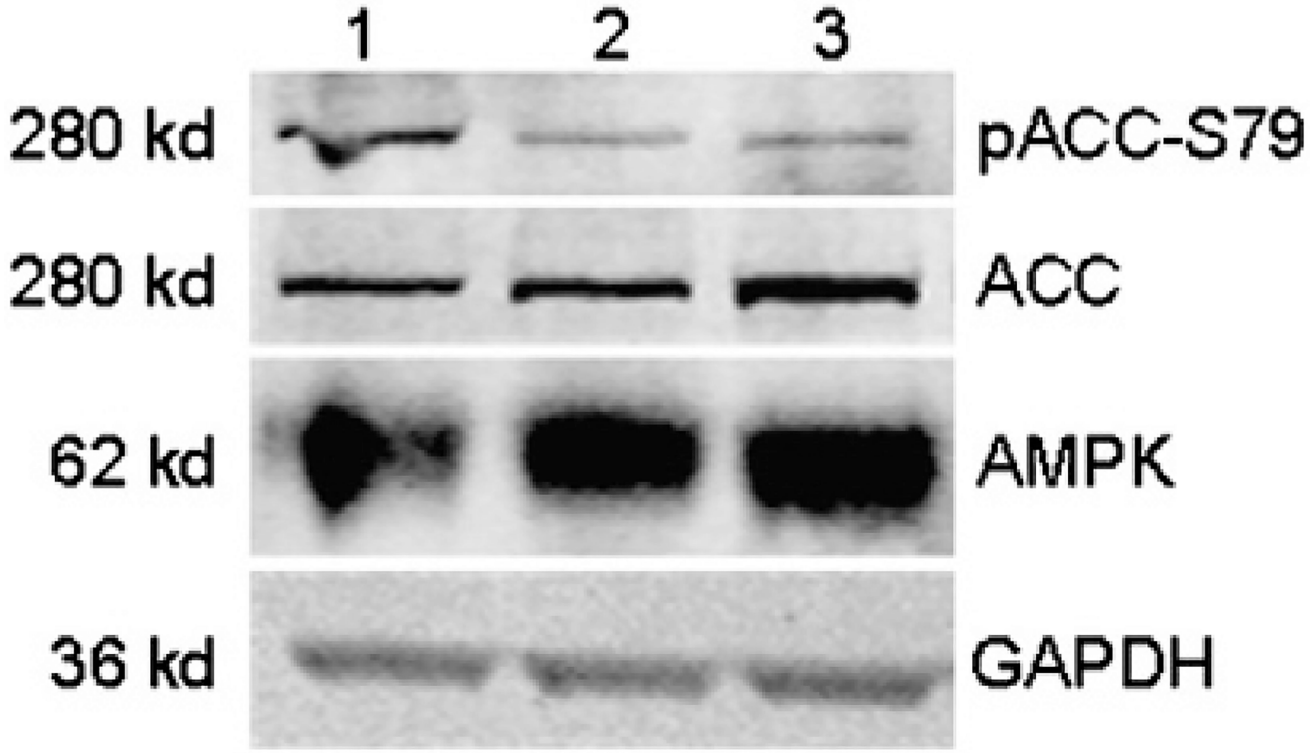

Fig. 4.

Validation of downstream signaling of AMPK kinase inhibitor in iPSC-CMs. iCell cardiomyocytes were treated with (1) vehicle, (2) 31 μM RO-3857 [AMPK], and (3) 15 μM sunitinib for 2 h. iCell whole cell lysates were subjected to Western blotting with antibodies specific to pACC-S79, ACC, AMPK, and GAPDH.

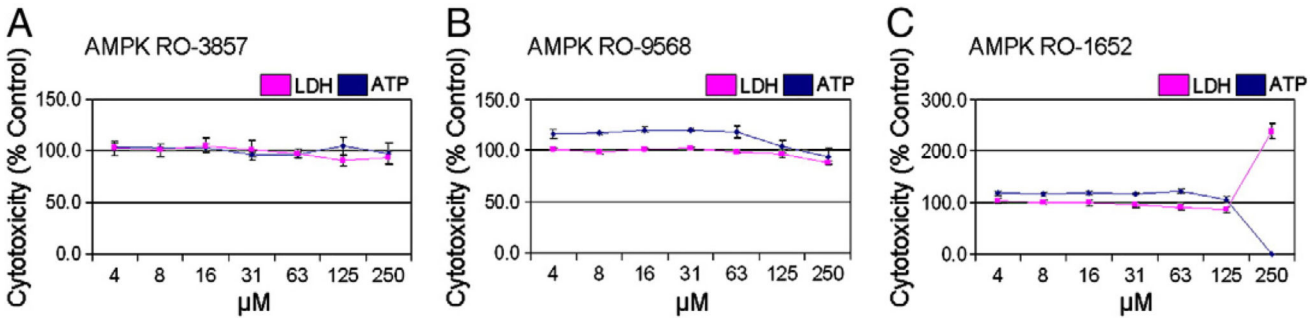

Fig. 5.

AMPK kinase inhibitors are not cardiotoxic in iPSC-CMs. iCell cardiomyocytes were treated for 24 h with 4 to 250 μMof (A–C) small molecule inhibitors of AMPKα1/2 (RO-3857, RO-9568, and RO-1652). iCells were then assayed for LDH release and ATP depletion. N=4 for all treatment groups.

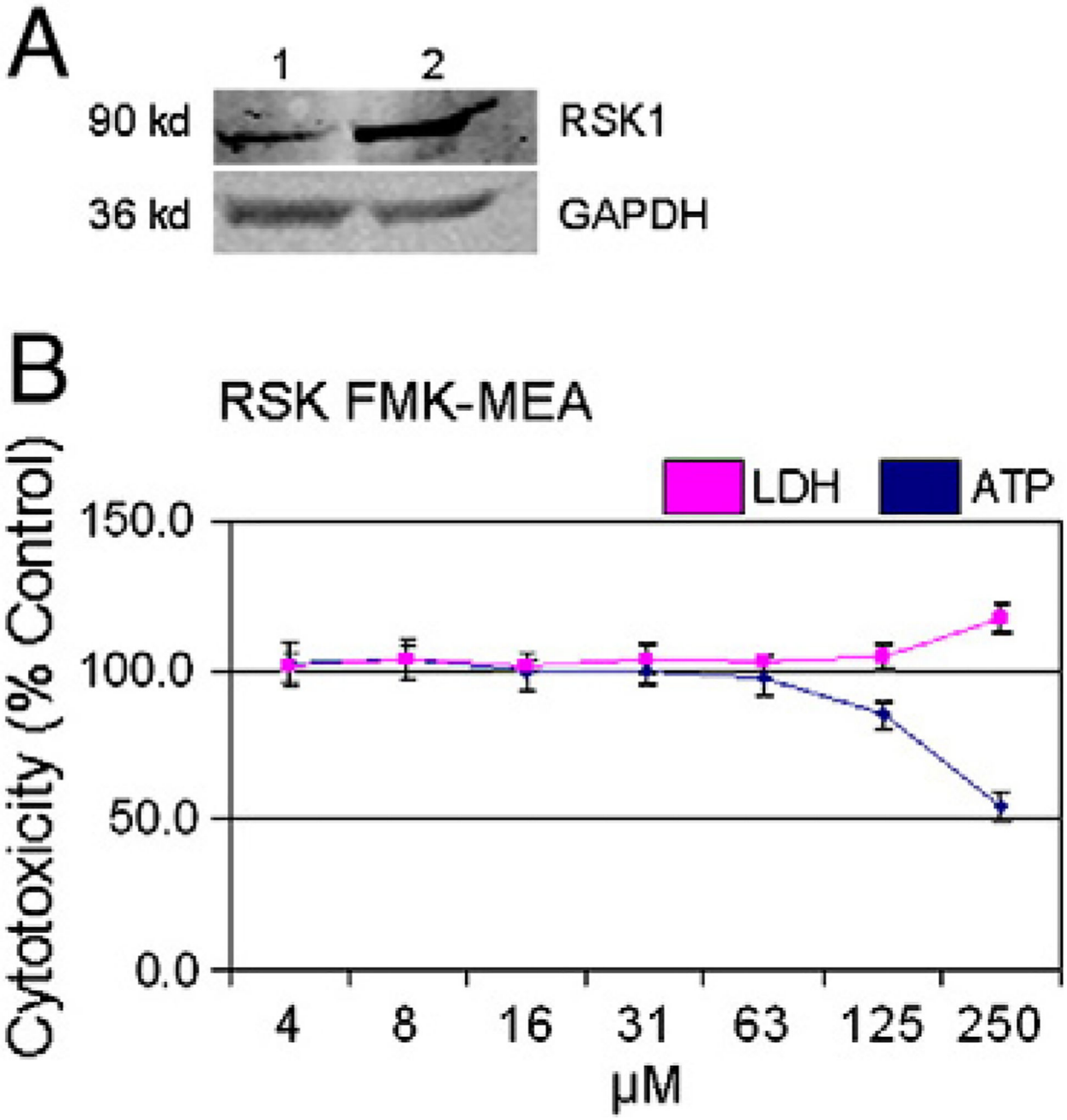

Fig. 6.

Irreversible RSK1/2/4 inhibitor is not cardiotoxic in iPSC-CMs. (A) iCell [1] and HEK293 [2] whole cell lysates were subjected to Western blotting with antibodies specific to RSK1 and GAPDH. (B) iCell cardiomyocytes were treated for 24 h with 4 to 250 μM of an irreversible RSK inhibitor (RSK FMK-MEA). iCells were then assayed for LDH release and ATP depletion. N=4 for all treatment groups.

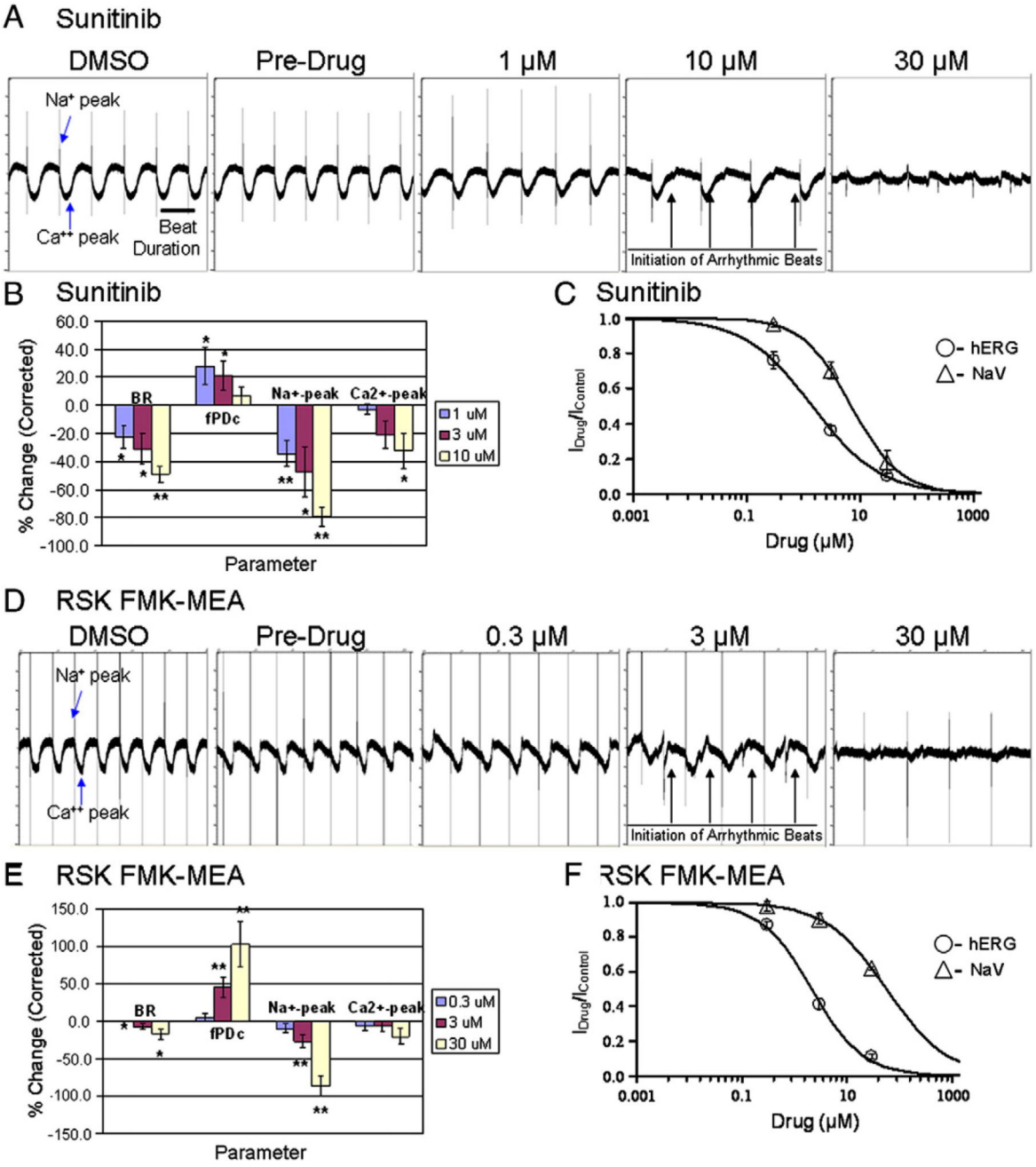

Fig. 7.

Sunitinib and RSK inhibitor-mediated electrophysiological changes in human iPSC-CMs. Human iPSC-CMs were plated on microelectrode arrays (MEA). (A) MEA traces representative of serially increasing additions of sunitinib (0, 1, 10, 30 μM) that were recorded for 15 min at each concentration, and each trace represents 10 s.". (B) Normalized beat rate (BR), field-potential duration (fPDc), sodium (Na^{+}) peak, and calcium (Ca^{2+}) peak of sunitinib MEA results. Mean ± SEM, n = 4 wells, * $p < 0.05$, ** $p < 0.01$ (*t*-test). (*C*) Using CHO-hERG and CHL-Nav1.5 cells, hERG and Nav1.5 channel assays were performed following serially increasing additions of sunitinib (0, 0.3, 3, 30 μM). n = 3 for

hERG, and n = 9 for Nav1.5. (D) MEA traces representative of serially increasing additions of RSK FMK-MEA (0, 0.3, 3, 30 μM) that were recorded for 15 min at each concentration. (E) Normalized beat rate (BR), field-potential duration (fPDc), Na^+ peak, and Ca^{2+} peak of RSK FMK-MEA results. Mean ± SEM, n = 4 wells, * $p < 0.05$, ** $p < 0.01$ (*t*-test). (F) Using CHO-hERG and CHL-Nav1.5 cells, hERG and Nav1.5 channel assays were performed following serially increasing additions of RSK FMK-MEA (0, 0.3, 3, 30 μM). N = 6 for hERG, and n = 3 for Nav1.5.

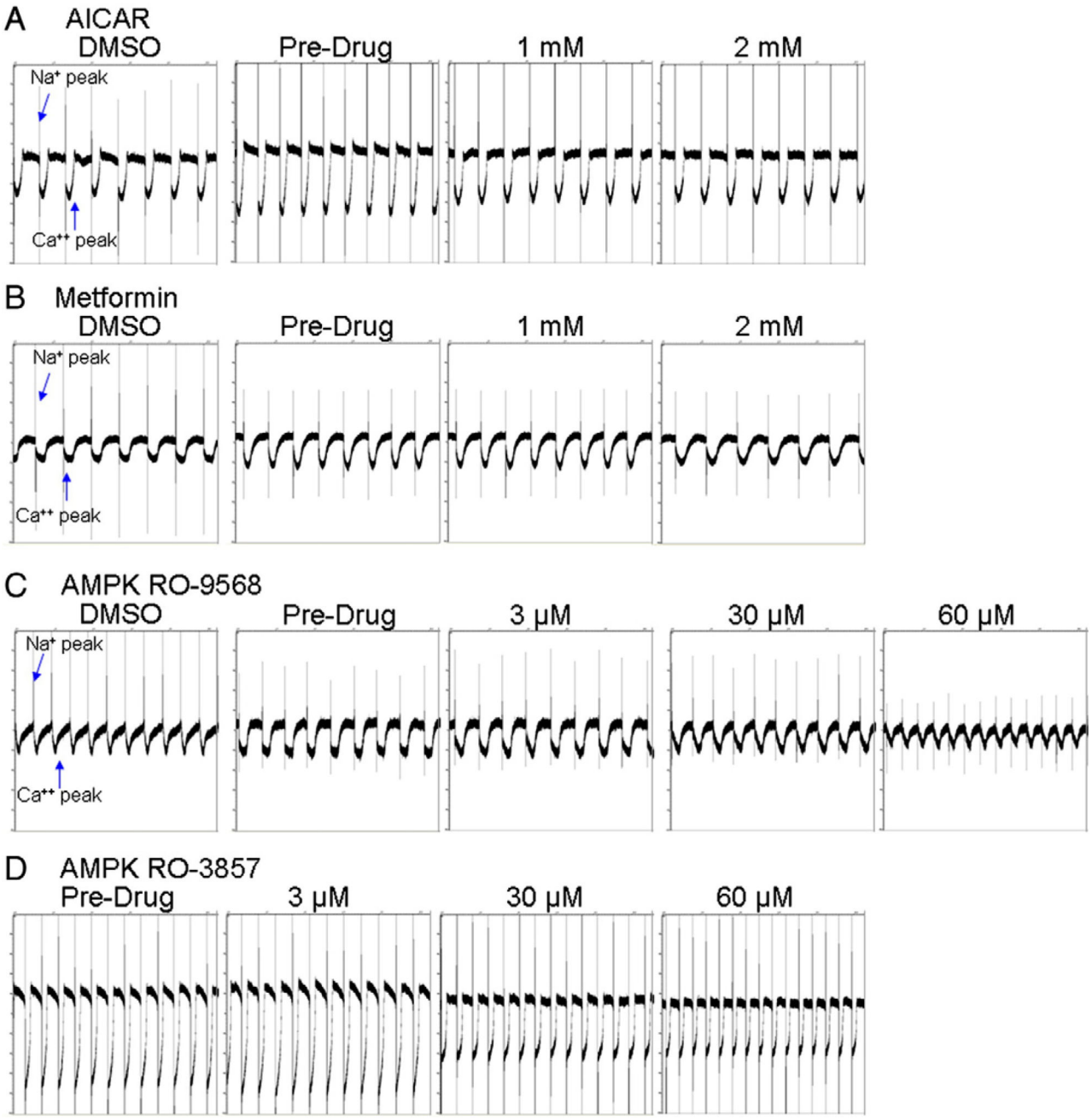

Fig. 8.

AICAR, metformin, and AMPK inhibitor-mediated electrophysiological changes in human iPSC-CMs. Human iPSC-CMs were plated on microelectrode arrays (MEA). MEA traces of serially increasing additions (0, 1, 2 mM) of (A) AICAR or (B) metformin that were recorded for 15 min at each concentration. MEA traces of serially increasing additions (0, 3, 30, 60 μM) of AMPK inhibitors (C) RO-9568 or (D) RO-3857 that were recorded for 15 min at each concentration, and each trace represents 10 s.”.

Table 1

Cardiac specific kinases predicted to be involved in mediating sunitinib cardiotoxicity.

A				B			
Kinases	**% Inhibition AMBIT**	**Kinases**	**% Inhibition AMBIT**	**Kinases**	**% Inhibition AMBIT**		
					RO-3857	RO-9568	RO-1652
AMP_K-alpha1	100	ROCK2	97				
AMPK-alpha2	99	ABL1	93	AMPK-alpha1	98	96	95
AURORA B KINASE	100	CDKL2	92	AMPK-alpha2	98	95	93
AURORA C KINASE	100	JAK2 (Kin. Dom.2)	92	CAMK2D	75	75	1
CDK7	100	AKT2	79	CDK7	1	1	69
KIT	100	ABL2	77	FLT3	74	1	72
PDGFR-alpha	100	PDPK1	71	KIT	86	84	79
PDGFR-beta	100	AKT3	<50.0	PDGRF-beta	70	78	93
PLK4	100	AURORA A KINASE	<50.0	RPS6KA1 (Kin. Dom.1)	1	90	99
FLT1	100	BRAF	<50.0	RPS6KA1 (Kin. Dom.2)	1	99	71
FLT3	100	DMPK	<50.0	RPS6KA2 (Kin. Dom.1)	92	1	97
FLT4	100	ERBB2	<50.0	RPS6KA3 (Kin. Dom.1)	71	89	84
VEGFR2	100	ERBB4	<50.0	RPS6KA4 (Kin. Dom.1)	69	83	1
STK11	100	GSK3A	<50.0	RPS6KA5 (Kin. Dom.1)	84	97	72
RPS6KA1 (Kin. Dom.1)	100	GSK3B	<50.0	RPS6KA6 (Kin. Dom.1)	1	91	78
RPS6KA2 (Kin. Dom.1)	100	MAP3K5 (ASK1)	<50.0	RPS6KA6 (Kin. Dom.2)	1	1	62
RPS6KA4 (Kin. Dom.1)	100	MAPK/ERK2	<50.0				
RPS6KA4 (Kin. Dom.2)	99	PIK3CA	<50.0				
RPS6KA5 (Kin. Dom.2)	98	PIK3CG	<50.0				
RPS6KA6 (Kin. Dom.1)	97	PIM1	<50.0				
RPS6KA5 (Kin. Dom.1)	94	PIM2	<50.0				
RPS6KA3 (Kin. Dom.1)	92	PLK1	<50.0				
RPS6KA1 (Kin. Dom.2)	84	PLK3	<50.0				
RPS6KA2 (Kin. Dom.2)	76	RAF	<50.0				
PTK2 (FAK)	99	RPS6KA6 (Kin. Dom.2)	<50.0				
CAMK2D	97						

(A) Kinases with known importance in cardiac function (Force and Kolaja, 2011) were compared to the 10 μM sunitinib AMBIT screen (Supplemental Fig. 1). The highlighted data (pink) represents the simplified list of kinases which may be involved in sunitinib mediated cardiotoxicity. (B) Kinases listed in (A) that were also inhibited by the AMPK inhibitors (RO-3857, RO-9568, and RO-1652) that were not cardiotoxic.